Available online at www.sciencedirect.com
ScienceDirect
Journal of the European Ceramic Society 28 (2008) 1057–1063
www.elsevier.com/locate/jeurceramsoc

# Properties of silicon nitride for aluminum melts prepared by nitrided pressureless sintering

In-Sub Han [a,*], Doo-Won Seo [a], Sei-Young Kim [a], Ki-Seog Hong [a], Kil Ho Guahk [b], Kee Sung Lee [b]

[a] *Energy Materials Research Center, Korea Institute of Energy Research (KIER), 71-2 Jangdong, Yusonggu, Daejon 305-343, Republic of Korea*
[b] *School of Mechanical and Automotive Engineering, Kookmin University, 861-1 Chongnungdong, Songbukgu, Seoul 136-702, Republic of Korea*

Available online 27 December 2007

**Abstract**

In this study, silicon nitride ceramics for aluminum melts were prepared by nitrided pressureless sintering (NPS) process, which process is the continuous process of nitridation reaction of Si metal combined with pressureless sintering. Mechanical, chemical and thermal properties of the NPS silicon nitride sintered with $Al_2O_3$, $Y_2O_3$ and Si additives were evaluated. Fully densed products show appropriate strength, ~500 MPa, high hardness, ~13 GPa, and superior damage tolerances with high fracture toughness, ~9.8 MPa $m^{1/2}$. Contact testing with spherical indenters is used to characterize the damage response. Examination of the indentation sites indicates a quasi-plastic damage modes are observed. Bend tests on specimens containing quasi-plastic contact damages reveal those materials to be not susceptible to strength degradation. And it has a low thermal expansion coefficient of $2.9 \times 10^{-6}$ °C, and good thermal conductivity of 28 W/mK.


*Keywords:* Silicon nitride; Nitrided pressureless sintering; Reaction sintering; Aluminum

## 1. Introduction

Silicon nitride ($Si_3N_4$) ceramics have been studied for several decades about forming, sintering, and microstructure control in high temperature and wear resistant applications because of attractive combination of mechanical and thermal properties.[1–4] $Si_3N_4$ can be used for bearing ball, motor valve, turbine rotor and cutting tool as an industrial structural component as well as rocket propulsion components, jig for semiconductor industry, RF window, and nano probes are of high interest at the present.[3,5–8] In the last several decades fully densified $Si_3N_4$ have been achieved by various sintering techniques such as reaction-bonding (RBSN), pressureless sintering (PS), hot press (HPSN), and gas pressure sintering (GPS).

Thermal, chemical and mechanical resistant ceramics including non-oxide ceramics are required for aluminum (Al) industry. Degassing pipe and rotor are used to stir molten aluminum and bubble gases for removal of hydrogen, because detrimental impurities remain such as $H_2$, Na or Ca component in the aluminum.[9,10] Degassing is conducted at high temperature, >700 °C in a refractory-lined box that contains 226.8–453.6 kg of aluminum at a time. The degassing pipe has an impeller at the end and it is rotated (200–600 rpm). Therefore $Si_3N_4$ degassing pipe and rotor blade are used in aluminum melts due to these superior thermal, chemical and mechanical properties.[9–11] However, one of the drawbacks is high cost in the preparation of $Si_3N_4$ components. It is generally accepted that high quality of structural $Si_3N_4$ ceramics can only be produced from submicron raw powders, under 1 μm, with high purity (>99.9%). Expensive conventional sintering process and diamond machining have restricted wider applications, especially in the molten aluminum industry. The other critical drawback is low reliability due to inferior fracture toughness rather than a commercial metal.

On the other hand, reaction-bonded $Si_3N_4$ (RBSN) is a way of producing cost effective one using relatively cheap Si powder instead of expensive $Si_3N_4$ powder even though the enhancement of mechanical properties are required.[12] To improve the mechanical properties of RBSN, NPS is replaceable new process because the mechanical properties of NPS silicon nitride can be much improved by post sintering at 1800–1820 °C. Moreover, the lower sintering temperature and almost no dimensional change in the 1st stage of sintering step have economical advantage. Even though several studies have been performed on the

* Corresponding author.
*E-mail address:* ishan@kier.re.kr (I.-S. Han).

0955-2219/$ – see front matter © 2007 Elsevier Ltd. All rights reserved.
doi:10.1016/j.jeurceramsoc.2007.09.032

NPS $Si_3N_4$,[9–11] there is no systematic study on the properties of NPS $Si_3N_4$.

Therefore, in this study, we utilized NPS (nitrided pressureless sintering) one-step process,[9–11] which can make cost-effective $Si_3N_4$ product using reaction-bonding process up to certain temperature, and obtain the dense sample with high mechanical properties by consequent pressureless sintering process at the final stage of heat treatment. In the present study, we investigate the mechanical properties such as four-point flexural strength, hardness, and fracture toughness. The contact damage response and strength degradation of the NPS $Si_3N_4$ are evaluated using spherical indenter.[13–18] Thermal properties such as thermal expansion coefficient and thermal conductivity are also measured. Additionally, the strength degradations of the NPS by corrosion medium are also checked. The results indicate that $Si_3N_4$ prepared by NPS process suggest the prospect of the application for degassing pipe and rotor blade with high thermal, mechanical and chemical resistance for molten aluminum industry.

## 2. Experimental

Experimental procedures for the fabrication of NPS silicon nitride ($Si_3N_4$) are shown in Fig. 1. The starting $Si_3N_4$ powders were relatively coarse α-$Si_3N_4$ (Saint-Gobain, China, mean particle size 2 μm, purity 95%). The starting Si powders used were recycled powders from semiconductor industry with high-purity (>99.9%) and consisted of 6 μm of mean particle size. $Al_2O_3$ (AKP-50, Sumitomo Chemical Co. Ltd., Japan) and $Y_2O_3$ (Fine Grade, H. C. Starck GmbH, Germany) powders were added for sintering additives. Sintering additives, $Y_2O_3$, $Al_2O_3$, Si with various compositions, 2A6Y5S, 4A6Y5S, and 5Y5A5S, were mixed with each starting powder. The powders were ball-milled in distilled water for 24 h. The milled powder was dried and sieved with a 150 μm screen. The detailed compositions of starting materials are summarized in Table 1.

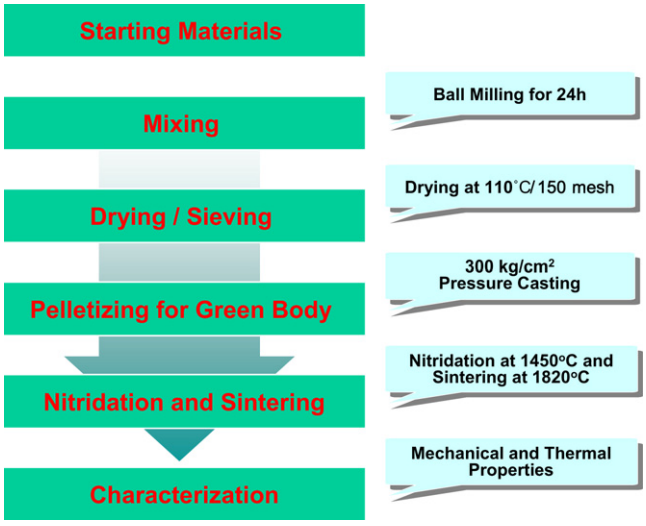


Fig. 1. Schematic diagram of the NPS process for preparing silicon nitride using in molten aluminum industry.

Table 1
Batch compositions and relative densities of NPS silicon nitrides

| Composition | $Si_3N_4$ (wt%) | Si (wt%) | $Al_2O_3$ (wt%) | $Y_2O_3$ (wt%) | Relative density (%) |
|---|---|---|---|---|---|
| 2A6Y5S | 95 | 5 | 2 | 6 | 82 |
| 4A6Y5S | 95 | 5 | 4 | 6 | 88.5 |
| 5A5Y5S | 95 | 5 | 5 | 5 | 99 |

The sieved powder was then pressed at a pressure of 30 MPa in a mold with a dimension 60 mm × 60 mm. During nitridation a heating rate of 3 °C/min was applied up to 1100 °C and then 0.5 °C/min to 1400–1450 °C. After that, the preforms were heated up to 1800–1820 °C at a rate of 5 °C/min and held for 3 h. In all of the runs, no packing powder was used. A nitrogen($N_2$) gas with 99.9% of purity was used for nitriding and constant gas pressure of 102.7–105.3 kPa was maintained. The sintered bodies were machined into rectangular bars of 4 mm × 4 mm × 25 mm for evaluating mechanical, thermal and chemical properties.

The sintered densities were measured using the Archimedes method. The phase of sintered products, were analyzed by X-ray diffractometer. The microstructure was examined by scanning electron microscopy (SEM, JEOL, JSM-6700F, Japan). The grain sizes were analyzed by linear intercepting method.

Strength tests were conducted on bar specimens in four-point flexure. A minimum of 10 specimens were cut, edge chamfered, and then fractured at a constant cross-head speed. Conventional Vickers indentations were performed for measuring hardness and toughness at load $P = 50$ N, on the polished surfaces.

Hertzian indention tests were carried out using a tungsten carbide (WC) spheres of radii $r = 1.98$, 2.38, 3.18 or 3.56 mm.[13–17] Indentation stress–strain curves were obtained from measurements of contact radius at each value of $P$ and $r$, with varying the load from 30 to 4000 N. Then the indentation stress, $p_o = P/\pi a^2$, and indentation strain, $a/r$ were calculated.[14,18] Strength degradation was evaluated by four-point flexural bending test after Hertzian indentation as shown in Fig. 2.[13] The contact damages were observed by optical microscopy in Nomarski illumination and SEM.

The NPS specimens were immersed in the corrosive condition separately, $H_2SO_4$, HCl, $HNO_3$, or NaOH solution (NaOH: $H_2O$ = 1:1) for a constant time. The exposed time was changed from 0 to 2000 h. Thermal expansion coefficients were measured using dilatometer (DIL 402C, Netzsch, Germany) in temperature range of 30–1400 °C. The thermal conductivity was calculated from measuring thermal diffusivity coefficient, $\alpha$, and specific heat $C_p$ measured using thermal diffusivity measurement instrument (TC-7000, Shinku-Riko, Japan) and specific heat measurement instrument (DSC-404C, Netzsch, Germany). The sintered bar specimens were also thermal shocked from 1300 °C to room temperature in air rapidly and maintained for 2 min. and then heated up to 1300 °C again and maintained for 2 min. Cooling fan was blown during the holding time in air. This cycle was repeated to 1000, 2000, 5000, 10 000 and 20 000 cycles for each sample. The flexural strength tests were run on the sintered bar

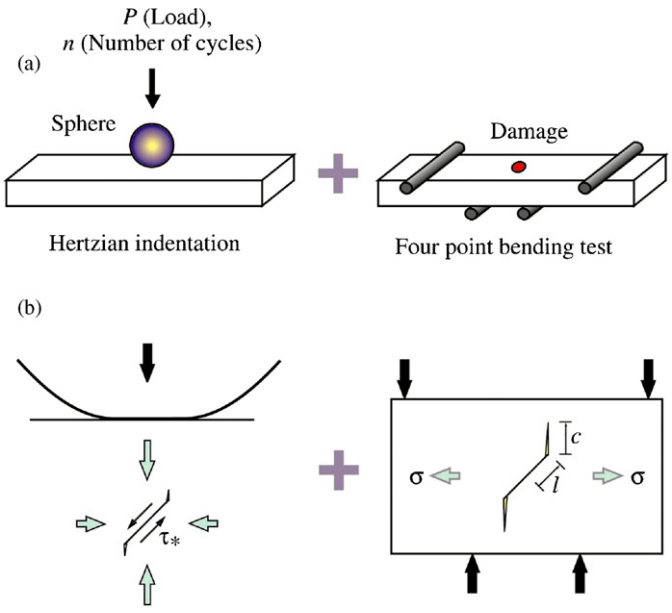


Fig. 2. Schematic diagram of Hertzian indentation and strength degradation test against damages produced by spherical indentation, (a) experimental set up and (b) stress acted on the microcracks on shear fault.

specimens before and after the exposure in the corrosive and thermal shock condition.

## 3. Results and discussion

### 3.1. Characteristics of NPS silicon nitride

Table 1 shows relative density data of the sintered NPS $Si_3N_4$ with different compositions of $Al_2O_3$ and $Y_2O_3$ additive at constant 5 wt% of Si content. The $Si_3N_4$ sintered with 2A6Y5S shows the lowest sintered density due to $Y_2O_3$ rich composition of the additive. On the other hand, it is noteworthy that the density increases by the increasing fraction of $Al_2O_3$ in the sintering additive. 5 wt% of Si addition in 5A5Y composition indicates that fully densified samples can be obtained using NPS process. The relative higher density in the NPS $Si_3N_4$ with 5A5Y5S additives are closely related with no weight change during the NPS reaction. It is conjectured that the oxide additives act as nitridation promoters of Si. The composition 5A5Y5S has the lowest eutectic point (higher diffusion of nitrogen), from that reason the conversion of Si to $Si_3N_4$, density and α–β phase

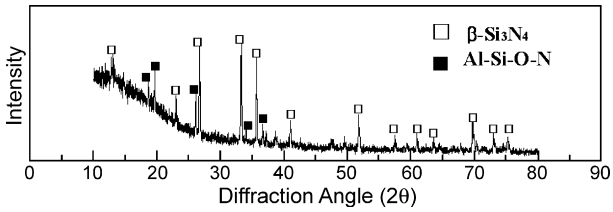


Fig. 4. XRD pattern of the NPS $Si_3N_4$ (5A5Y5S). Each peak is designated by □ β-$Si_3N_4$ and ■ Al–Si–O–N.

transformation is the highest. On the other hand, the 4–5 wt% of weight loss found in 2A6Y5S and 4A6Y5S compositions indicate the Si may be vaporized for the compositions by the reaction of $N_2$ gas with $SiO_2$ existing on the $Si_3N_4$ or Si powders before solution-reprecipitation mechanism occurs during reaction sintering.

Fig. 3 represents SEM micrographs of the NPS $Si_3N_4$ with different types of sintering additives, 2A6Y5S, 4A6Y5S, 5A5Y5S. While the porous microstructures were observed for the $Si_3N_4$ with 2A6Y5S and 4A6Y5S compositions, the $Si_3N_4$ with 5A5Y5S composition showed uniform and dense microstructure by increasing the fraction of $Al_2O_3$ in the starting composition. After NPS process, this material reveals a microstructure with prismatic β elongated grains as shown in Fig. 3(c). The micrograph implies that the sintered products by NPS process have uniform microstructure that containing similar sizes of β elongated grains.

Fig. 4 shows the XRD pattern of 5A5Y5S sample with major β-$Si_3N_4$ phase and with minor peaks of Al–Si–O–N crystalline phases.

### 3.2. Mechanical properties and contact damages of NPS silicon nitride

We have evaluated the mechanical properties and contact damage tolerance of the 5Y5A5S NPS $Si_3N_4$ because the results of sintered density, XRD and SEM analysis indicate these materials are highly dense and contain elongated β grains (Table 2).

Table 3 summarizes the mechanical properties of the NPS $Si_3N_4$. The strength and hardness of the NPS $Si_3N_4$ is high enough for application as degassing pipe and rotor, $\sigma_{o,max} > 500$ MPa and $H_{max} = 12.6$ GPa. It is noteworthy that NPS $Si_3N_4$ shows high fracture toughness, relative to commercial $Si_3N_4$, which shows 3.9–7.0 MPa $m^{1/2}$.

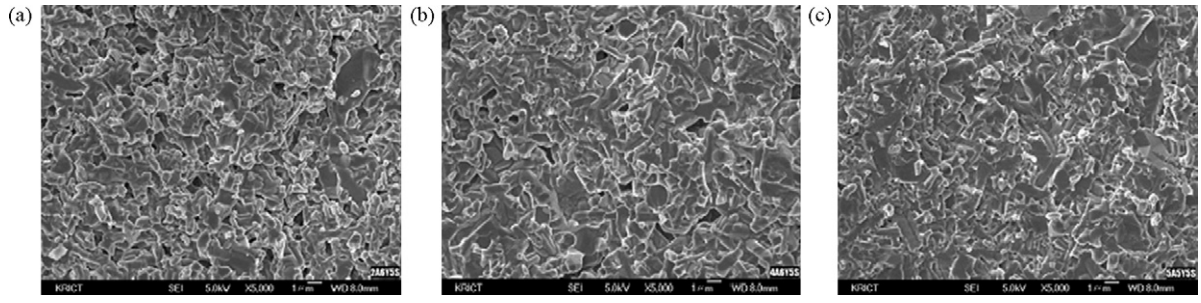


Fig. 3. SEM micrographs of the NPS $Si_3N_4$ with different amounts of sintering additives, (a) 2A6Y5S, (b) 4A6Y5S and (c) 5A5Y5S. The detailed compositions are indicated in Table 1.

Table 2
NPS silicon nitride (5A5Y5S) data for evaluation of mechanical properties

| Description | Data |
|---|---|
| Sintering additive | 5 wt% $Al_2O_3$ 5 wt%$Y_2O_3$ 5 wt% Si (5A5Y5S) |
| Nitridation/sintering condition | 1450 °C, 1 h/1820 °C, 3 h in $N_2$ 770–790 mmHg |
| Relative density(%) | 99 |
| Grain morphology | Elongated |
| Grain size, diameter/length(μm) | $0.54 \pm 0.06/3.5 \pm 0.3$ |
| β-Phase (vol%) | 100 |

Table 3
Mechanical properties of NPS silicon nitride (5A5Y5S)

| Description | Data | Max data |
|---|---|---|
| Hardness, $H$ (GPa) | 1214 ± 47 | 1261 |
| Toughness, $T$ (MPa $m^{1/2}$) | 7.8 ± 2.0 | 9.8 |
| Strength, $\sigma_o$ (MPa) | 442 ± 58 | 500 |

Indentation stress–strain data of NPS $Si_3N_4$ is shown in Fig. 5. In this figure the solid curve is best curve fit from data. The NPS $Si_3N_4$ shows slight nonlinearity in the stress–strain curve. The indentation stress–strain curve showed similar behavior with samples fabricated using hot pressing sintering process shown in our previous study.[1]

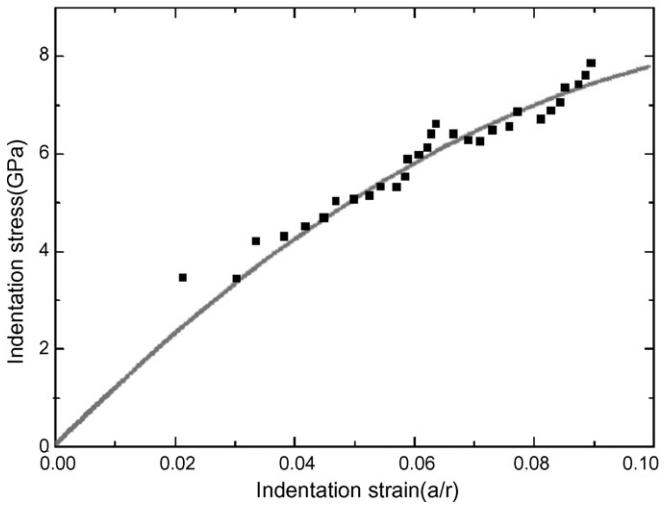


Fig. 5. Indentation stress–strain curves of the NPS $Si_3N_4$ with 5 wt% $Al_2O_3$, 5 wt% $Y_2O_3$ and 5 wt% Si additives (5A5Y5S).

Data for the strengths $\sigma_F$ are plotted as a function of contact load $P$ in Fig. 6. The horizontal solid lines denote, "laboratory" or "inert" strengths, $\sigma_o$, of unindented specimens. Open symbols indicate specimens that broke away from indentation sites. Dark symbols represent symbols that broke at indentation sites. It is reported that the mode of contact damages change as the grain sizes of ceramic material become coarser and more heterogeneous, and consequently tougher, undergo-

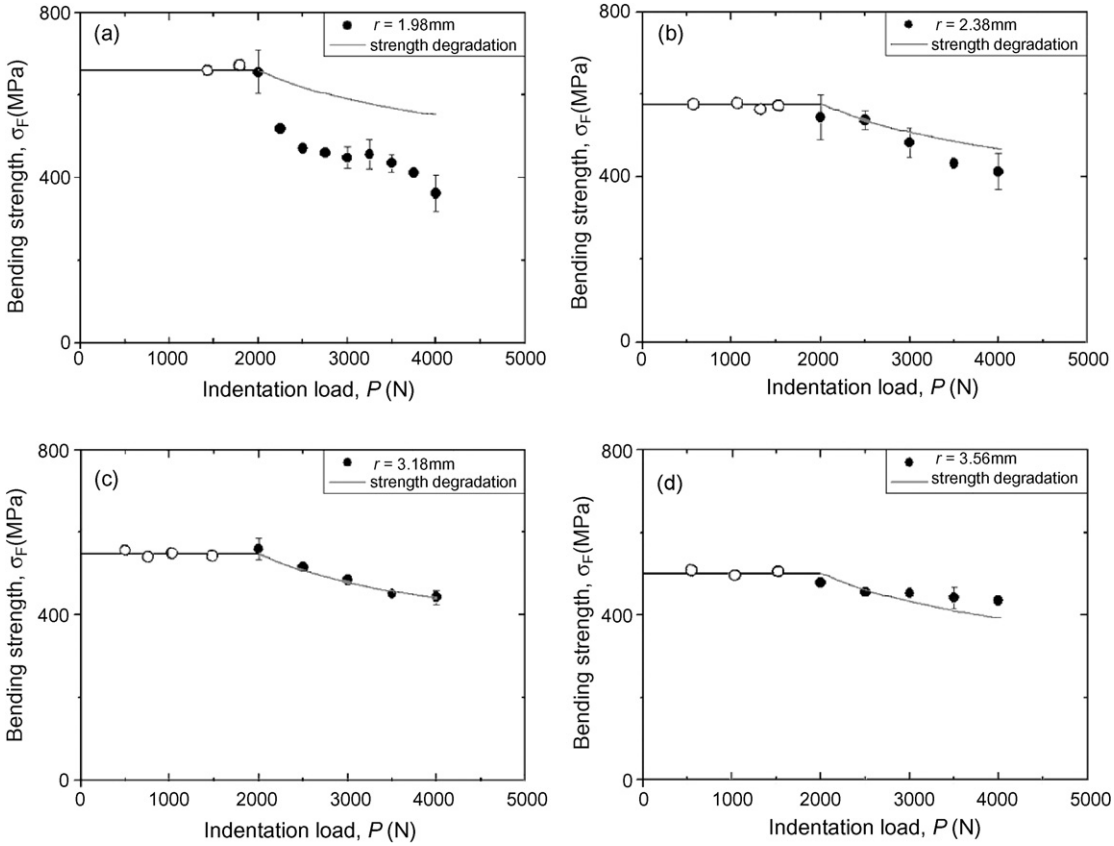


Fig. 6. Strengths of NPS $Si_3N_4$ after spherical indentation using different radius of WC sphere, (a) 1.98 mm, (b) 2.38 mm, (c) 3.18 mm and (d) 3.56 mm. The lines from strength degradation model[13] are included in each graph.

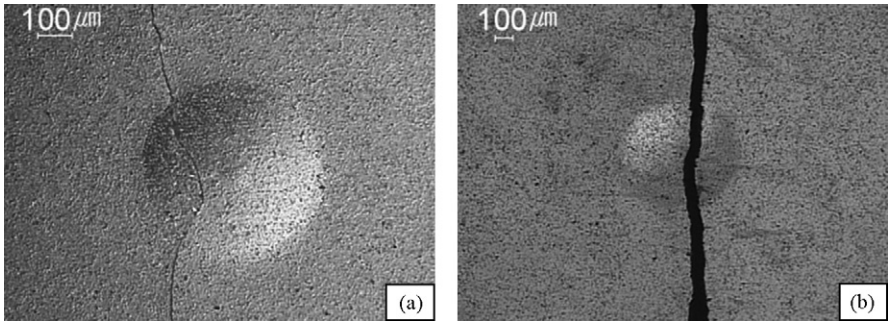


Fig. 7. Surface views of contact failure sites after spherical indentation with (a) WC sphere radius $r = 1.98$ mm at load $P = 2250$ N and (b) $r = 3.56$ mm at load $P = 4000$ N, in the NPS $Si_3N_4$. The views are observed in Nomarski illumination of optical microscope.

ing a "brittle-to-quasi-plastic" transition[13,14,16,17]: in coarse-β grain heterogeneous microstructures exhibit diffuse microdamage forms in the region of strong compression-shear stress beneath the contact point rather than ring or cone cracks. In heterogeneous microstructures, failure occurs from single shear fault/wing cracks within the damage zone as shown in Fig. 1(b), whereas the strength degradation is gradual than in homogeneous ceramics, where abrupt strength losses occur beyond the critical load for cone crack initiation. The model[13] implies that strength can be evaluated from $P_D$, the load when the strength degradation starts, $P_Y$, the load when the quasi-plasticity begins, and each indentation load, $P$. The strength correspond to the mean laboratory strength $\sigma_o$ at $P < P_D$, but at $P \geq P_D$,

$$\sigma_F = \sigma_o \left[ \frac{P_D^{1/3} - P_Y^{1/3}}{P^{1/3} - P_Y^{1/3}} \right]^{1/3} \quad (1)$$

The solid lines are theoretical fits from the strength degradation model by Eq. (1). The data of strength shows slight strength degradation occurs by quasi-plastic damage. It is notable that the experimental results are comparatively coincided with the theoretical fits as the blunt spheres are used. Thus the quasi-plasticity mode happened in the NPS $Si_3N_4$ is less deleterious to strength than commercial $Si_3N_4$.[2,14,17]

Fig. 7 shows the representative fracture origins produced in the NPS $Si_3N_4$. The figure shows failure origins on broken strength test specimens containing indentation damages from WC spheres, (a) $r = 1.98$ mm, at load $P = 2250$ N and (b) $r = 3.56$ mm, at load $P = 4000$ N. Failure modes are indicated by peripheral fracture paths tangent to the damages. All fracture paths in the NPS $Si_3N_4$ pass through the damaged quasi-plastic yielded zone. This phenomenon indicates that fracture originated from the flaw in the subsurface damage zone as shown in the schematic diagram of Fig. 1(b).

Therefore the results in Figs. 6 and 7 indicates that the failure behavior of the NPS $Si_3N_4$ is quasi-ductile behavior found in heterogeneous microstructures,[13,14,16,17] indicating the strength does not degraded abruptly during indentation.

### 3.3. Chemical and thermal properties of NPS silicon nitride

The results of strength degradation tests by immersing in corrosive fluids, are shown in Fig. 8. The graph plots the strength data as a function of holding time for corrosion tests, at room temperature in the selected solution as indicated in the graph, $H_2SO_4$, HCl, $HNO_3$ or NaOH. The exposure time was varied to 2000 h. Data points are the average value of three data. It is important to study the effect of corrosive component because the component can be exposed in degassing process of molten aluminum industry. It is found that the strength falls off slightly at an initial cycle by corrosion. However, it is noteworthy that the strength degradation is not significant relative to the inert laboratory strength of the NPS $Si_3N_4$ before corrosion tests. As degassing pipe and rotor component is operated at high temperature,[8–11] hot corrosion study is currently investigated.

The thermal expansion coefficient for the NPS $Si_3N_4$, 5A5Y5Si composition, is shown in Fig. 9(a). Low thermal expansion coefficients, $2.23–2.89 \times 10^{-6}\,K^{-1}$ were measured, respectively. Low thermal expansion coefficient does not build up residual tensile stress by mismatch with that of aluminum melts during repetitive heating and cooling cycle. Thus, it is expected that the NPS $Si_3N_4$ can be stably used even at high temperature.

The maximum thermal conductivity of the $Si_3N_4$ prepared by NPS with 5A5Y5Si additive was 28 W/m K as shown in Fig. 9(b). This good thermal conductivity is related with micro-sized pores in the sintered body as shown in Fig. 3. The strengths after longtime thermal shock tests plotted in Fig. 10 suggests

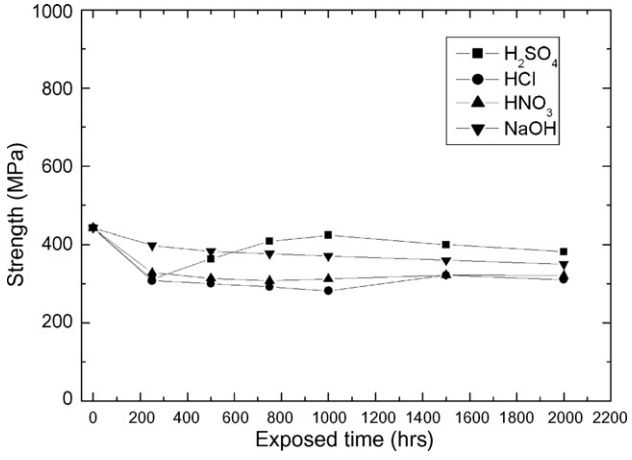


Fig. 8. Flexural strength of the NPS $Si_3N_4$ (5A5Y5S) as a function of holding time in corrosive fluid at room temperature.

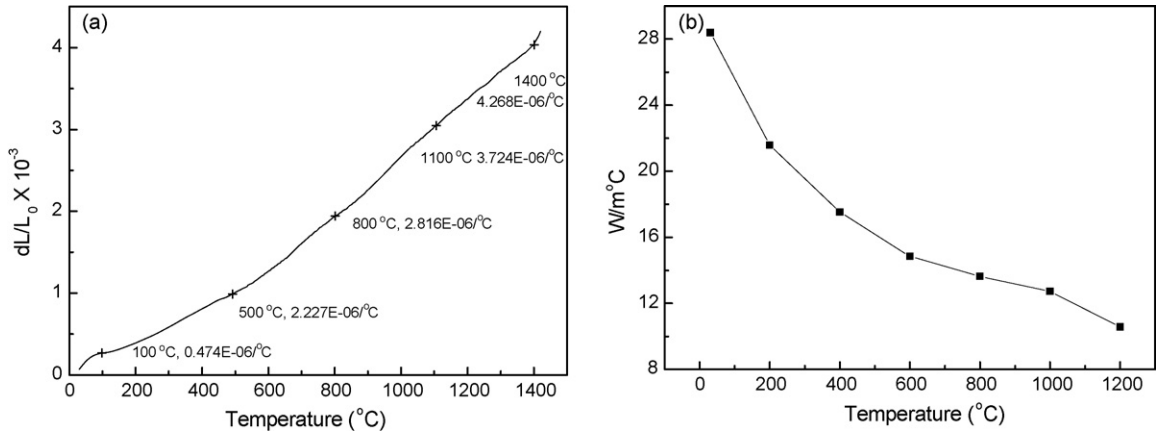


Fig. 9. Thermal properties of the NPS $Si_3N_4$, (a) thermal expansion coefficients and (b) thermal conductivity of 5A5Y5S as a function of temperature.

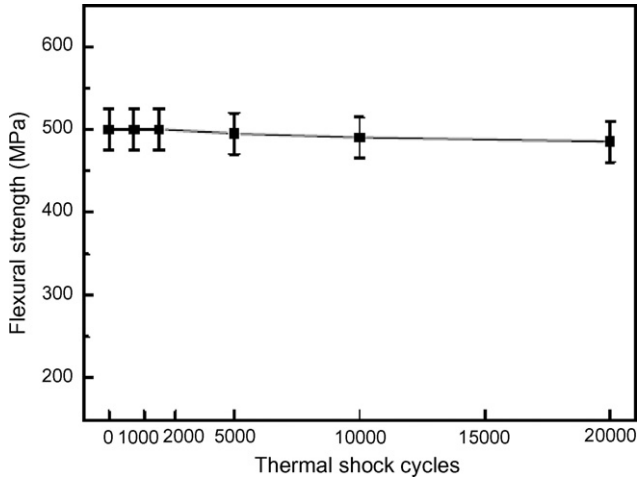


Fig. 10. Flexural strength of the NPS $Si_3N_4$ as a function of thermal shock cycles, after thermal shock tests are conducted on 5A5Y5S.

high thermal stability of the $Si_3N_4$ prepared by NPS in this study. The graph indicates that the $Si_3N_4$ with 5A5Y5Si composition have superior thermal stability in the thermal shock condition,[19] between 30 and 1300 °C, up to 20 000 cycles.

## 4. Conclusions

$Si_3N_4$ ceramics have been prepared by low cost nitrided pressureless sintering (NPS) process using different amounts of Si, $Al_2O_3$ and $Y_2O_3$ additives. Mechanical, chemical and thermal properties of fully dense 5A5Y5S sample were evaluated. The evaluation of mechanical properties indicate that the NPS $Si_3N_4$ showed appropriate mechanical properties, strength 500 MPa, hardness 12.6 GPa, and superior fracture toughness 9.8 MPa $m^{1/2}$. Contact damages by spherical indentations and the strength degradation tests showed high damage-tolerant properties with slight strength degradation by quasi-plastic contact damages. It was confirmed that the NPS $Si_3N_4$ has high thermal stability in the thermal shock condition up to 20 000 cycles due to lower thermal expansion and good thermal conductivity.

## Acknowledgement

This research was supported by a grant from the Energy Resources Technology Development Programs funded by the Korea Energy Management Corporation of the Ministry of Commerce, Industry and Energy of Korean government.

## References

1. Lee, S. K., Wuttiphan, S. and Lawn, B. R., Role of microstructure in Hertzian contact damage in silicon nitride. 1: Mechanical characterization. *J. Am. Ceram. Soc.*, 1997, **80**, 2367–2381.
2. Lee, S. K. and Lawn, B. R., Role of Microstructure in Hertzian contact damage in silicon nitride: II, Strength degradation. *J. Am. Ceram. Soc.*, 1998, **81**, 997–1003.
3. Mukerji, J. and Prakash, B., Wear of nitrogen ceramics and composites in contact with bearing steel under oscillating sliding condition. *Ceramics International*, 1998, **24**, 19–24.
4. Riley, F. L., Silicon nitride and related materials. *J. Am. Ceram. Soc.*, 2000, **83**, 245–265.
5. Moulson, A. J., Reaction-bonded silicon nitride: Its formation and properties. *J. Mater. Sci.*, 1979, **14**, 1017–1021.
6. Lee, S. Y., Fabrication of $Si_3N_4$/SiC composite by reaction-bonding and gas pressure sintering. *J. Am. Ceram. Soc.*, 1998, **81**, 1262–1268.
7. Lin, H. T. and Ferber, M. K., Mechanical reliability evaluation of silicon nitride ceramic components after exposure in industrial gas turbines. *J. Am. Ceram. Soc.*, 2002, **22**, 2789–2797.
8. Huang, H., Winchester, K. J., Suvorova, A., Lawn, B. R., Liu, Y., Hu, X. Z. *et al.*, Effect of deposition conditions on mechanical properties of low-temperature PECVD silicon nitride films. *Mater. Sci. & Eng.*, 2006, **A435–36**, 453–459.
9. Han, I. S., Cheon, S. H., Chung, Y. H., Seo, D. W., Lee, S. W., Woo, S. K. *et al.*, Preparation and properties of silicon nitride ceramics by nitrided pressureless sintering (NPS) process. *Key Eng. Mater.*, 2006, **317–318**, 125–130.
10. Richerson, D. W., Industrial applications of ceramic matrix composites. In *Comprehensive Composite Materials*, *Vol. 6*, ed. A. Kelly and C. Zweben. Elsevier, Amsterdam, 2000, pp. 549–570 [Chapter 6.28].
11. Brown, I. W. M., Pompe, R. and Carlsson, R., Preparation of sialons by the nitrided pressureless sintering (NPS) technique. *J. Eur. Ceram. Soc.*, 1990, **6**, 191–200.
12. Han, I. S., Lee, K. S., Seo, D. W. and Woo, S. K., Improvement of mechanical properties in RBSC by boron carbide addition. *J. Mater. Sci.*, 2002, **21**, 703–706.
13. Lawn, B. R., Lee, S. K., Peterson, I. M. and Wuttiphan, S., Model of strength degradation from Hertzian contact damage in tough ceramics. *J. Am. Ceram. Soc.*, 1998, **81**, 1509–1520.

14. Lawn, B. R., Indentation of ceramics with spheres: A Century after Hertz. *J. Am. Ceram. Soc.*, 1998, **81**, 1977–1994.
15. Lee, K. S., Wuttiphan, S., Hu, X. Z., Lee, S. K., Lawn, B. R. and Lawn, Contact-induced transverse fractures in brittle layers on soft substrates: A study on silicon nitride bilayers. *J. Am. Ceram. Soc.*, 1998, **81**, 571–580.
16. Lee, S. K., Lee, K. S., Lawn, B. R. and Kim, D. K., Effect of starting powder on damage resistance of silicon nitrides. *J. Am. Ceram. Soc.*, 1998, **81**, 2061–2070.
17. Lee, K. S., Lee, K., Lawn, B. R. and Kim, D. K., Contact damage and strength degradation in brittle/quasi-plastic silicon nitride bilayers. *J. Am. Ceram. Soc.*, 1998, **81**, 2394–2404.
18. Hu, X. Z. and Lawn, B. R., A simple indentation stress–strain relation for contacts with spheres on bilayer structures. *Thin Solid Films*, 1998, **322**, 225–232.
19. Lee, S. K., Moretti, D. and Readey, M. J., and Lawn B. R., Thermal shock resistance of silicon nitrides using an indentation-quench test. *J. Am. Ceram. Soc.*, 2002, **85**, 279–281.